Supporting Information: Band edge exciton in CdSe and other II-VI and III-V compound semiconductor nanocrystals – Revisited

Peter C. Sercel*,† and Alexander L. Efros*,‡

†*T. J. Watson Laboratory of Applied Physics, California Institute of Technology, Pasadena, California 91125, USA*

‡*Naval Research Laboratory, Washington DC 20375, USA*

E-mail: psercel@caltech.edu; efros@nrl.navy.mil

Band edge exciton wave functions and energies

We chose the Bloch functions $u^c_{1/2,\pm 1/2}$ of the Γ_6 conduction band and $u_{3/2,\mu}$ ($\mu = \pm 3/2, \pm 1/2$) of the Γ_8 valence band (point group T_d) according to Ref.[1]:

$$u^c_{1/2,1/2} = S\uparrow, \quad u^c_{1/2,-1/2} = S\downarrow, \tag{S1}$$

and

$$u_{3/2,3/2} = -\frac{1}{\sqrt{2}}(X+iY)\uparrow, \qquad u_{3/2,-3/2} = \frac{1}{\sqrt{2}}(X-iY)\downarrow,$$
$$u_{3/2,1/2} = \frac{1}{\sqrt{6}}\left[-(X+iY)\downarrow + 2Z\uparrow\right], \qquad u_{3/2,-1/2} = \frac{1}{\sqrt{6}}\left[(X-iY)\uparrow + 2Z\downarrow\right]. \tag{S2}$$

Here S and X, Y, Z are the orbital Bloch functions for the s-type and p-type band edge symmetry, respectively. The spinor functions $\uparrow$ and $\downarrow$ are the eigenfunctions of the electron spin projection operator $s_z = \pm 1/2$.

The electron wave functions for the electron ground state $1S_{\rm e}$ level in a spherical NC can be written as

$$\Psi^{\rm e}_{s_z}(\mathbf{r}) = R_{\rm e}(r) Y_{00} u^c_{1/2,s_z}\,, \tag{S3}$$

where spherical harmonic, $Y_{00}(\theta,\phi) = 1/\sqrt{4\pi}$, and $R_{\rm e}(r) = \sqrt{2/a}\sin(\pi r/a)/r$ is the normalized radial function, where a is the NC radius and r is the radial coordinate. The first size-quantization level of holes in a spherical NC is a $1S_{3/2}$ state[2,3] characterized by total angular momentum $F = 3/2$ and is four-fold degenerate with respect to its projection $M = 3/2, 1/2, -1/2, -3/2$ on the z axis. The wave functions of this state can be written in the hole representation as[4]

$$\Psi^{1S_{3/2}}_M(\boldsymbol{r}) = 2\sum_{l=0,2}(-1)^{M-3/2}(i)^l R_l(r) \sum_{m+\mu=M} \begin{pmatrix} l & 3/2 & 3/2 \\ m & \mu & -M \end{pmatrix} Y_{l,m} u_{3/2,\mu}\,. \tag{S4}$$

Here $\left(\begin{smallmatrix} i & k & l \\ m & n & p \end{smallmatrix}\right)$ are the Wigner 3j-symbols, and the spherical angular harmonics $Y_{lm}(\theta,\phi)$ are defined in Ref.[5]. Note, that the factor $(i)^l$ introduced because we use the definition of spherical harmonics Y_{lm} as given in Ref.[5] while in Ref.[4] the spherical harmonics were defined according to Ref.[6]. The radial wave functions R_0 and R_2 in Eq.(S4) are given by:

$$R_0(r) = A\left(j_o(k_{hh}r) - \frac{j_o(k_{hh}a)}{j_o(k_{lh}a)} j_o(k_{lh}r)\right),\ R_2(r) = -A\left(j_2(k_{hh}r) + \frac{j_o(k_{hh}a)}{j_o(k_{lh}a)} j_2(k_{lh}r)\right). \tag{S5}$$

where $k_{lh} = \sqrt{\beta} k_{hh}$ and $k_{hh} = \sqrt{m_{hh}\epsilon_{1S_{3/2}}}/\hbar$ are connected with the energy of the $1S_{3/2}$ level $\epsilon_{1S_{3/2}}$ determined by equation: $j_0(k_{hh}a)j_2(k_{lh}a) + j_0(k_{lh}a)j_2(k_{hh}a) = 0$.[2,7] Here $\beta = m_{lh}/m_{hh}$ is the ratio of the light, m_{lh}, to the heavy, m_{hh}, hole effective masses and the constant A is determined from the normalization condition $\int \left[R_0^2(r) + R_2^2(r)\right] r^2 dr = 1$.

For the $1P_{3/2}$ hole state the wave function can be written as:

$$\Psi_M^{1P_{3/2}} = 2\sum_{l=1,3}(-1)^{M-3/2}(i)^l R_l(r)\sum_{m+\mu=M}\begin{pmatrix} l & 3/2 & 3/2 \\ m & \mu & -M \end{pmatrix} Y_{l,m}u_{3/2,\mu} \ , \tag{S6}$$

where the radial wavefunctions for these states are given by,

$$R_1(r) = 3B\left(j_1(k_{hh}r) - \frac{j_1(k_{hh}a)}{j_1(k_{lh}a)}j_1(k_{lh}r)\right), \ R_3(r) = -B\left(j_3(k_{hh}r) + 9\frac{j_1(k_{hh}a)}{j_1(k_{lh}a)}j_3(k_{lh}r)\right), \tag{S7}$$

where $k_{hh} = \sqrt{m_{hh}\epsilon_{1SP3/2}}/\hbar$ are connected with the energy of the $1P_{3/2}$ level $\epsilon_{1P_{3/2}}$, determined by equation: $9j_1(k_{hh}a)j_3(k_{lh}a) + j_1(k_{lh}a)j_3(k_{hh}a) = 0$ and the constant B is set by the normalization condition, $\int \left[R_1^2(r) + R_3^2(r)\right] r^2 dr = 1$. As described in the main text, the quantum size level energy difference between the $1P_{3/2}1S_e$ and $1S_{3/2}1S_e$ excitons, in the absence of fine structure splitting or Coulomb corrections, was calculated using the 6-band model, expressions for which are derived in Ref. 3, rather than using the 4-band expressions for the QSL energies. Use of the 4-band expressions causes a 57 meV error in the QSL energy at the smallest radius calculated, $a = 1.2$ nm, relative to the 6-band expressions, which is unacceptably large. However, using the 4-band wavefunctions creates a much smaller error of ~ 12meV in the Coulomb corrections at $a = 1.2$nm radius, while greatly simplifying the analytical expressions.

Short range exchange interaction

The short range electron–hole exchange interaction between an electron and a hole can be written following Ref.[8] as

$$\hat{H}_{\rm exch}^{SR} = \frac{2}{3}\varepsilon_{\rm exch}a_0^3\left[\frac{3}{2}\mathbb{I} - (\boldsymbol{\sigma}_e\cdot\boldsymbol{J})\right]\delta(\boldsymbol{r}_e - \boldsymbol{r}_h) \ , \tag{S8}$$

where $\varepsilon_{\rm exch}$ is the short range exchange constant, a_0 is the lattice constant and $\boldsymbol{J}$ is the spin matrix of the momentum $J = 3/2$. Eq.(S8) describes the absolute position of the exciton fine structure levels in the bulk relative to the energy of the bulk exciton in the absence of exchange, in contrast with Ref.[9], where only the splitting of the exciton fine structure levels was calculated. One can see from Eq.(S8) that the lowest bulk exciton state with total momentum $|(1/2)\boldsymbol{\sigma}_e + \boldsymbol{J}| = 2$ is not affected by the electron hole exchange interaction.[10]

Straightforward averaging of Eq. (S8) over the wave functions of the $1S_{3/2}1S_e$ confined exciton states results in the Hamiltonian of Eq.(1) of the main text, where the exchange constants $\eta^{SR}_{1S_{3/2}1S_e}$ and $\overline{\eta}^{SR}_{1S_{3/2}1S_e}$ are defined through dimensionless constants $\chi_{1S_{3/2}1S_e}(\beta)$ and $\overline{\chi}_{1S_{3/2}1S_e}(\beta)$, respectively:[9,10]

$$\chi_{1S_{3/2}1S_e} = \frac{a^3}{12}\int_0^a drr^2 R_{\rm e}^2(r)[R_0^2(r) + \frac{1}{5}R_2^2(r)] \ , \ \overline{\chi}_{1S_{3/2}1S_e} = \frac{a^3}{10}\int_0^a drr^2 R_{\rm e}^2(r)R_2^2(r) \ , \quad \text{(S9)}$$

These constants depend only on the ratio of light to heavy hole effective masses, β.

For the $1P_{3/2}1S_e$ exciton manifold the averaging of Eq.(S8) over the wave function of the $1S_e1P_{3/2}$ exciton states result in the Hamiltonian of Eq.(9) of the main text, where the exchange constants $\eta^{SR}_{1P_{3/2}1S_e}$ and $\overline{\eta}^{SR}_{1P_{3/2}1S_e}$ are defined through dimensionless constants $\chi_{1P_{3/2}1S_e}(\beta)$ and $\overline{\chi}_{1P_{3/2}1S_e}(\beta)$, respectively:[10,11]

$$\begin{aligned}
\chi_{1P_{3/2}1S_e} &= \frac{a^3}{12}\int_0^a drr^2 R_{\rm e}^2(r)\frac{[11R_1^2(r) - 9R_3^2(r)]}{15} \ , \\
\overline{\chi}_{1P_{3/2}1S_e} &= \frac{a^3}{8}\int_0^a drr^2 R_{\rm e}^2(r)\frac{[4R_1^2(r) + 24R_3^2(r)]}{15} \ . \qquad \text{(S10)}
\end{aligned}$$

Long range exchange interaction

The non-analytic, or long-range, part of the electron hole exchange interaction between an electron and a hole can be written following the approach outlined by Ajiki and Cho.[12] This approach, developed initially for homogeneous bulk semiconductors, was generalized

to quantum dots in the strong confinement regime.[13] According to Ajiki and Cho[12] any given exciton state is accompanied by a transition dipole density $\boldsymbol{P}(\boldsymbol{r})$ and consequently an optically induced charge density $\rho(\boldsymbol{r}) = -(\nabla_{\boldsymbol{r}} \cdot \boldsymbol{P}(\boldsymbol{r}))$. The long range exchange interaction can be written as the Coulomb energy of this optically induced charged density:[14]

$$H_{exch}^{LR} = \int d^3r_1 \int d^3r_2 (-\nabla_{\boldsymbol{r}_1} \cdot \boldsymbol{P}(\boldsymbol{r}_1))^* U(\boldsymbol{r}_1, \boldsymbol{r}_2)(-\nabla_{\boldsymbol{r}_2} \cdot \boldsymbol{P}(\boldsymbol{r}_2)) \ , \tag{S11}$$

where $U(\boldsymbol{r}_1, \boldsymbol{r}_2)$ is the Coulomb interaction. For a bulk semiconductor, $U(\boldsymbol{r}_1, \boldsymbol{r}_2) = e^2/(\epsilon_{in}|\boldsymbol{r}_1 - \boldsymbol{r}_2|)$ with Coulomb charge e screened by the bulk semiconductor dielectric constant, ϵ_{in}. However, in a semiconductor NC, the Coulomb interaction should include corrections due to the dielectric discontinuity at the NC surface. These corrections can be viewed as the interaction between the electron and the hole with the image charges associated with the other carrier. We write these corrections generically as $V_{im}(\boldsymbol{r}_1, \boldsymbol{r}_2)$:

$$U(\boldsymbol{r}_1, \boldsymbol{r}_2) = \frac{e^2}{\epsilon_{in}|\boldsymbol{r}_2 - \boldsymbol{r}_1|} + V_{im}(\boldsymbol{r}_1, \boldsymbol{r}_2) \ . \tag{S12}$$

To calculate the exchange interaction using Eq.(S11) we will express the two terms within Eq.(S12) in a multipole expansion appropriate for spherical geometry. For spherical NCs one can write,

$$U(\mathbf{r_1}, \mathbf{r_2}) = \frac{1}{\epsilon_{in} a} \sum_{l,m} C_l^m(r_1, r_2) Y_l^{m*}(\theta_1, \phi_1) Y_l^m(\theta_2, \phi_2), \tag{S13}$$

where $C_l^m(r_1, r_2)$ is a function of the radial coordinates only, and is given by,

$$C_l^m(r_1, r_2) \equiv \frac{4\pi}{(2l+1)} \left[\frac{a r_<^l}{r_>^{l+1}} + \frac{(\epsilon_{in} - \epsilon_{out})(l+1)}{[\epsilon_{in} l + \epsilon_{out}(l+1)]} \left(\frac{r_1 r_2}{a^2} \right)^l \right] \ , \tag{S14}$$

ϵ_{out} is the dielectric constant of surrounded medium and $r_>$ or $r_<$ is the greater or lessor value of r_2 or r_1. The first term in Eq.(S14) originates from the usual direct Coulomb multipole expansion[15] while the second term represents the corrections associated with the dielectric discontinuity at the NC surface.[16]

In the strong confinement limit, when the exciton Bohr radius is larger than the NC radius, a, the wave function of the exciton is just the direct product of the electron and hole wave functions: $\Psi_{s_z,M}(\boldsymbol{r}_e,\boldsymbol{r}_h)=\Psi^{\rm e}_{s_z}(\boldsymbol{r}_e)\Psi^{3/2}_{M}(\boldsymbol{r}_h)$ defined in Eqs. (S3), (S4) and (S6). In this case the dipole density connected with a transition between one of the M hole states and one of s_z electron states can be written:

$$\boldsymbol{P}_{s_z,M}(\boldsymbol{r}_e)=i\frac{e}{m_0\omega}\int d^3r_h\langle\hat{T}[\Psi^{3/2}_{M}(\boldsymbol{r}_h)]|\hat{\boldsymbol{p}}_e|\Psi^{\rm e}_{s_z}(\boldsymbol{r}_e)\rangle\delta(\boldsymbol{r}_e-\boldsymbol{r}_h)\ , \tag{S15}$$

where m_0 is the mass of a free electron, ω is the transition frequency, $\hat{T}$ is the time-reversal operator, and $\hat{\boldsymbol{p}}_e$ is the momentum operator that acts only on the Bloch component of the electron and hole wave function. The eight components ($2\times4=8$) of the transition dipole density $\boldsymbol{P}_{s_z,M}(\boldsymbol{r}_e)$ between a $1S_e$ electron and a $1S_{3/2}$ or $1P_{3/2}$ hole level results in an 8×8 matrix representation of the long range exchange Hamiltonian, $\hat{H}^{LR}_{exch}$, defined in Eq. (S11), for the corresponding sub-space.

Results for the $1S_{3/2}1S_e$ exciton manifold

Substituting Eq. (S15) into Eq.(S11) and using hole wave functions from Eq.(S4) leads, after some cumbersome but straightforward calculations, to the long-range exchange Hamiltonian that we determined for the $1S_{3/2}1S_e$ exciton manifold:[10]

$$\hat{H}^{LR}_{1S_{3/2}1S_e}=\eta^{LR}_{1S_{3/2}1S_e}\left[\frac{3}{2}\mathbb{I}-(\boldsymbol{\sigma}\cdot\boldsymbol{F})\right]\ . \tag{S16}$$

The exchange constant, $\eta^{LR}_{1S_{3/2}1S_e}$ in Eq.(S16) can be written as,

$$\eta^{LR}_{1S_{3/2}1S_e}=\frac{\hbar\omega_{LT}}{4}\left(\frac{a_{ex}}{a}\right)^3\left[\xi_{1S_{3/2}1S_e}(\beta)+\left(\frac{\epsilon_{in}-\epsilon_{out}}{\epsilon_{in}+2\epsilon_{out}}\right)\frac{2|Q^{(1)}_0(\beta)|^2}{3}\right]\ . \tag{S17}$$

In Eq.(S17) $\hbar\omega_{LT}$ is the bulk longitudinal-transverse splitting for wurzite semiconductors:

$$\hbar\omega_{LT} = \frac{2E_p}{\epsilon_{in}a_{ex}^3}\frac{\hbar^2e^2}{m_0E_g^2} \ , \tag{S18}$$

where E_p is the Kane energy parameter, E_g is the bulk energy gap, a_{ex} is the Bohr radius of the bulk exciton and m_0 is the mass of free electron. The dimensionless functions $\xi_{1S_{3/2}1S_e}(\beta)$ and $Q_0^{(1)}(\beta)$ are defined as a sum of integrals involving the electron and hole radial functions:

$$\xi_{1S_{3/2}1S_e}(\beta) \equiv \frac{1}{27}\left(I_{0,0}^{(1)} - 2I_{0,2}^{(1)} + I_{2,2}^{(1)}\right) \ , \tag{S19}$$

where,

$$\begin{aligned}
I_{0,0}^{(1)} &= \int_0^1 x_1^2dx_1\int_0^1 x_2^2dx_2\left(\frac{x_<}{x_>^2}\right)q_0'(x_1)q_0'(x_2) \\
I_{0,2}^{(1)} &= \int_0^1 x_1^2dx_1\int_0^1 x_2^2dx_2\left(\frac{x_<}{x_>^2}\right)q_0'(x_1)\left(3\frac{q_2(x_2)}{x_2} + q_0'(x_2)\right) \\
I_{2,2}^{(1)} &= \int_0^1 x_1^2dx_1\int_0^1 x_2^2dx_2\left(\frac{x_<}{x_>^2}\right)\left(3\frac{q_2(x_1)}{x_1} + q_0'(x_1)\right)\left(3\frac{q_2(x)}{x_2} + q_0'(x_2)\right) \ .
\end{aligned} \tag{S20}$$

Here the dimensionless integrand functions $q_L(x)$ and $q_L'(x)$ are expressed via the radial functions R_0 and R_2 defined in Eq. (S5) as $q_L(x) \equiv \sqrt{2\pi^2}j_0(\pi x)a^{3/2}R_L(x)$ and $q_L'(x) \equiv dq_L(x)/dx$. The other dimensionless function, associated with the dielectric corrections, can be written as the dimensionless integral,

$$Q_0^{(1)}(\beta) \equiv \int_0^1 x^2dx\ q_0(x) = \sqrt{2\pi^2}\ a^{3/2}\int_0^1 x^2dx\ j_0(\pi x)R_0(x) \ . \tag{S21}$$

The expressions Eq.(S20) and Eq.(S21) only involve contributions from the $l = 1$ terms within Eq. (S13).

We have verified that the expressions above, derived using the method of Ajiki and Cho,[12] reduce to the corresponding expressions derived by Gouplav and Ivchenko using k-space integration.[17]

Results for the $1P_{3/2}1S_e$ excited state manifold

Applying the expressions above to determine the long-range exchange corrections within the $1P_{3/2}1S_e$ exciton manifold we find that all of the exchange corrections are associated with the $l = 2$ multipole in Eq.(S13). Performing the integrations as described previously we find the expression for the long-range exchange interaction within the $1P_{3/2}1S_e$ excited state manifold:

$$\hat{H}^{LR}_{1P_{3/2}1S_e} = \eta^{LR}_{1P_{3/2}1S_e}\left[\frac{5}{2}\mathbb{I} + (\boldsymbol{\sigma}_e \cdot \boldsymbol{F})\right] . \tag{S22}$$

The exchange constant, $\eta^{LR}_{1P_{3/2}1S_e}$ in Eq. (S22),

$$\eta^{LR}_{1P_{3/2}1S_e} = \frac{\hbar\omega_{LT}}{4}\left(\frac{a_{ex}}{a}\right)^3\left[\xi_{1P_{3/2}1S_e}(\beta) + \left(\frac{\epsilon_{in}-\epsilon_{out}}{2\epsilon_{in}+3\epsilon_{out}}\right)\frac{|Q^{(2)}_1|^2(\beta)}{5}\right] , \tag{S23}$$

is expressed via dimensionless integrals $\xi_{1P_{3/2}1S_e}(\beta)$ and $Q^{(2)}_1(\beta)$. The function $\xi_{1P_{3/2}1S_e}(\beta)$ can be written as,

$$\xi_{1P_{3/2}1S_e} \equiv \frac{1}{375}\left(I^{(2)}_{1,1} + 6I^{(2)}_{1,3} + 9I^{(2)}_{3,3}\right) , \tag{S24}$$

where,

$$\begin{aligned}
I^{(2)}_{1,1} &= \int_0^1 x_1^2 dx_1 \int_0^1 x_2^2 dx_2 \left(\frac{x^2_<}{x^3_>}\right)\left(\frac{q_1(x_1)}{x_1} - q_1'(x_1)\right)\left(\frac{q_1(x)}{x_2} - q_1'(x_2)\right) \\
I^{(2)}_{1,3} &= \int_0^1 x_1^2 dx_1 \int_0^1 x_2^2 dx_2 \left(\frac{x^2_<}{x^3_>}\right)\left(\frac{q_1(x_1)}{x_1} - q_1'(x_1)\right)\left(4\frac{q_3(x)}{x_2} + q_3'(x_2)\right) \\
I^{(2)}_{3,3} &= \int_0^1 x_1^2 dx_1 \int_0^1 x_2^2 dx_2 \left(\frac{x^2_<}{x^3_>}\right)\left(\frac{4q_3(x_1)}{x_1} + q_3'(x_1)\right)\left(4\frac{q_3(x)}{x_2} + q_3'(x_2)\right) .
\end{aligned} \tag{S25}$$

Here the functions $q_L(x)$ are defined now via radial functions R_1 and R_3 from Eq. S7. The other radial integral, associated with the dielectric corrections, can be written,

$$Q^{(2)}_1(\beta)\int_0^1 x^3 dx\; q_1(x) = \sqrt{2\pi^2}\; a^{3/2}\int_0^1 x^3 dx\; j_0(\pi x) R_1(x) . \tag{S26}$$

The effect of the long range exchange interaction and crystal field splitting on the oscillator transition strength.

The relative oscillator transition strength of the upper versus lower optically allowed transitions depends on the splitting between the heavy- and light-holes, Δ, defined in Eq. [2] of the main text, and the magnitude of the exchange constant, $\eta_{1S_{3/2}1S_e} = \eta^{SR}_{1S_{3/2}1S_e} + \eta^{LR}_{1S_{3/2}1S_e}$. As described in the main text, the relative transition strengths of the optically allowed transitions $\pm 1^U$, $\pm 1^L$ and 0^U can be calculated using Eq. 28 from Ref.[9] by replacing $\eta^{SR}_{1S_{3/2}1S_e}$ by the total value $\eta_{1S_{3/2}1S_e} = \eta^{LR}_{1S_{3/2}1S_e} + \eta^{SR}_{1S_{3/2}1S_e}$.

The experimental size dependence of the relative oscillator transition strength of the sum of the $\pm 1^U$ and 0^U exciton lines and the energetically lower $\pm 1^L$ exciton line, reported in Ref.[18], are shown in Fig.S1. In the same panel we show the result of calculations with and without including the long range exchange interaction. The dashed lines in the figure were calculated using a fixed internal crystal field, where the splitting Δ_{int} of the $1S_{3/2}$ hole level is proportional the bulk crystal field splitting Δ_{cr}: $\Delta_{int} = \Delta_{cr} v_{1S_{3/2}}(\beta)$. The dimensionless function $v_{1S_{3/2}}(\beta)$ is defined and plotted versus mass ratio β in Ref.[9]. Using the light- to heavy-hole mass ratio of CdSe ($\beta = 0.275$),[3] it has the value $v_{1S_{3/2}}(0.275) = 0.915$. The solid curves, labelled Δ_{ex} in the figure, include, in addition to the fixed internal crystal field term Δ_{int}, the shape anisotropy term Δ_{sh} for ellipsoidal NCs.[19] These were calculated using the experimentally determined size variation of the nanocrystal ellipticity for the samples measured in Refs.[9,18]. For reference, in Fig.S2, we plot Δ_{int}, the splitting connected with the hexagonal internal crystal field, Δ_{sh}, reflecting the contribution of the experimental NC shape, and the total splitting, $\Delta_{ex} = \Delta_{int} + \Delta_{sh}$. The experimentally determined size variation of the NC ellipticity, μ, is plotted on the right-hand vertical axis of Fig.S2. The ellipticity versus radius was calculated using a polynomial fitting expression to the experimental measurements of the size and shape, provided in note 30 of Ref.[9].

One can see in Fig.S1 that the model which includes long-range exchange as well as

the experimental shape distribution clearly represents a much better quantitative match to the measured oscillator strength data than the original model of Ref.[9], where long-range exchange was neglected. Moreover, the calculations which neglect the shape anisotropy term Δ_{sh} completely fail to describe the experimentally measured oscillator strength with either exchange model. This is because the fabricated NCs were significantly prolate, with measured ellipticity, μ, (defined in Ref.[19]) increasing from +0.03 at radius 1.2nm to +0.32 at radius 5nm. This creates a significant effect by reducing the total Δ, with a maximum reduction, $\Delta_{sh} = -11.8$meV occurring at a radius 2nm (see Fig. S2). Because the oscillator strength of the lower transitions decreases as Δ decreases for a given exchange constant, this effect must be accounted for in quantitative modelling of the optical transition strength of non-spherical NCs.

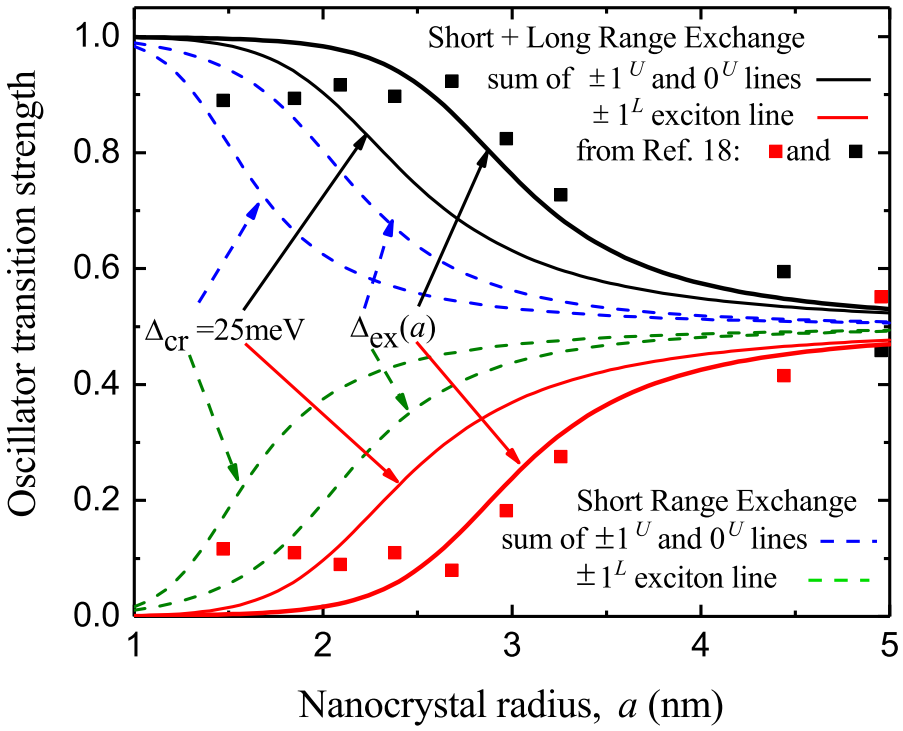

Figure S1: The relative oscillator transition strengths calculated with and without the long range exchange interaction are compared with the experimental results of Ref.[18] for various models of the light-heavy hole splitting Δ described by Eq.[2] of the main text. Curves labelled $\Delta_{cr} = 25$ meV were calculated for spherical shaped NCs with fixed bulk crystal field splitting parameter $\Delta_{cr} = 25$meV. The curves labelled Δ_{ex} include, in addition to the bulk crystal field splitting, the splitting connected with the NC shape anisotropy Δ_{sh}.[19] The total experimental splitting $\Delta_{ex} = \Delta_{int} + \Delta_{sh}$ used in calculating these curves takes into account the experimentally determined size variation of the NC ellipticity (see note 30 in Ref.[9]), which is plotted in Fig. S2, along with the calculated values of Δ_{int} and Δ_{sh}.

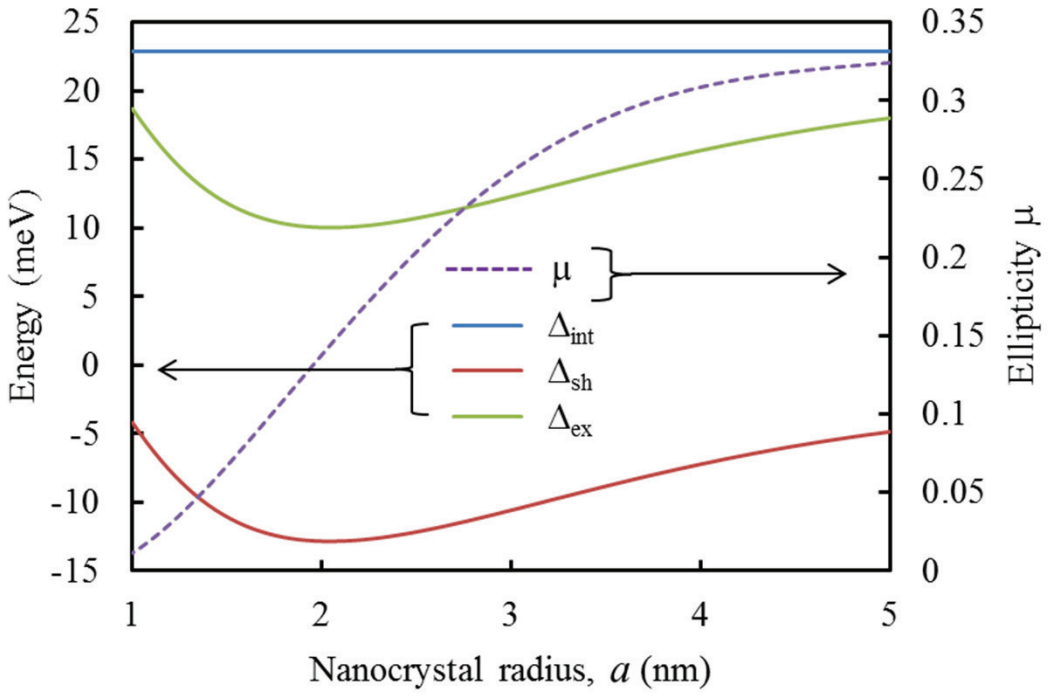

Figure S2: Splitting parameters calculated using the experimentally determined size variation of the ellipticity, μ, of the CdSe nanocrystal samples measured in Refs.[9,18]. The total splitting, $\Delta_{ex} = \Delta_{int} + \Delta_{sh}$, is plotted against the left-hand vertical axis. This parameter takes into account the contribution, Δ_{int}, of the hexagonal internal crystal field, and Δ_{sh}, reflecting the contribution of the experimental NC shape; these parameters are also plotted against the left-hand vertical axis for reference. The experimentally determined size variation of the NC ellipticity, μ, is plotted on the right-hand vertical axis. The ellipticity versus radius was calculated using a polynomial fitting expression to the experimental measurements of the size and shape, provided in note 30 of Ref.[9].

Supporting References

(1) Ivchenko, E. L. *Optical Spectroscopy of Semiconductor Nannostructures* (Alpha Science International Ltd., Harrow, UK, 2005) .

(2) Efros, Al. L.; Rodina, A. V. *Solid State Commun.* **1989**, *72*, 645-648.

(3) Ekimov, A. I.; Hache, F.; Schanne-Klein, M. C.; Ricard, D.; Flytzanis, C.; Kudryavtsev, I. A.; Yazeva, T. V.; Rodina, A.V.; Efros, Al. L. *J. Opt. Soc. Am. B.* **1993**, *10*, 100-107.

(4) Gel'mont, B. L.; D'yakonov, M. I. Sov. Phys. Semicond. **1972**, *5*, 1905- 1909.

(5) Edmonds, A. R. *Angular momentum in Quantum mechanics*, Princenton University Press, 1957.

(6) Landau, L.D.; Lifshitz, E.M. *Quantum Theory*, 2nd ed. (Pergamon, Oxford, 1965).

(7) Sercel P. C.; Vahala, K. J. *Phys. Rev. B.* **1990**, *42,* 3690 -3710.

(8) Bir, G. L.; Pikus, G. E. *Symmetry and Strain-Induced Effects in Semiconductors* John Wiley and Sons: New York, 1974.

(9) Efros, Al. L.; Rosen, M.; Kuno, M.; Nirmal, M.; Norris, D. J.; Bawendi, M. G. *Phys. Rev B* **1996**, *54*, 4843-4856.

(10) Sercel P. C. to be published.

(11) Sercel, P. C.; Shabaev, A.; Efros, Al. L. *Nano Lett.* **2017**, *17*, 4820-4830.

(12) Ajiki H.; Cho, K. *Proceedings of the Third International Conference on Excitonic Processes in Condensed Matter*, Boston, 1998, edited by R. T. Williams and W. M. Yen (Electrochemical Society, Pennington, NJ, 1999) p. 262.

(13) Ajiki H.; Cho, K. *International Journal of Modern Physics* **2001**, *15*, 3745-3748.

(14) Cho, K. *J. Phys. Soc. Japn.* **1999**, *68*, 683-691.

(15) Jackson, J. D. *Classical Electrodynamics*; John Wiley and Sons: New York, 1999.

(16) Kirkwood, J. G. *J. Chem. Phys.* **1934**, *2*, 351-361.

(17) Gupalov, S. V.; Ivchenko, E. L. *Phys. Sol. State* **2000**, *42*, 2030 -2038.

(18) Norris, D.; Efros, Al. L.; Rosen, M.; Bawendi, M. *Phys. Rev. B* **1996**, *53*, 16347-16354.

(19) Efros, Al. L.;Rodina, A.V. *Phys. Rev. B.* **1993**, *47*, 10005-10007.